Unmanned Aerial System for First Responders

Zachary Cook[1], Lin Zhao[1] and Jameson Lee[1], Woosoon Yim[1]
[1] Department of Mechanical Engineering, University of Nevada, Las Vegas, USA
(Tel : +1 702-895-0956; E-mail: woosoon.yim@unlv.edu)

Abstract - In this paper a roadmap is described for future work using stereo thermal cameras to locate and avoid heat sources or hot-spots commonly encountered in disaster remediation tasks using unmanned aerial vehicles (UAV). The proposed stereo forward looking infrared (FLIR) camera system will allow a UAV to locate bodies of heat, avoid such bodies to protect its sensitive mechanical and electronic components, and identify those heat sources globally in an objective frame in order to aid remote flight operators in the mapping of unknown and often hazardous environments. The locations of these identified bodies of heat can be combined with more traditional sensors used for obstacle detection such as LIDAR or a Time of Flight (ToF) camera to allow first responders to deploy UAV in many different types of emergency events. First responders can easily operate UAVs semi-autonomously to gather information, and act decisively without having to provide obstacle free paths for UAVs in advance. A 3D vector mesh (VM) avoidance algorithm will be used with sensor data from the stereo FLIR cameras, LIDAR, and the ToF camera to achieve both physical and thermal obstacle avoidance. The combination of these avoidance measures will facilitate the creation of a robust and semi-autonomous UAV platform that may provide critical support to first responders in typical disaster remediation tasks.

Keywords **- UAV, Stereo, FLIR Camera, Obstacle Avoidance**

1. Introduction

The aim of this research is to enhance the situational awareness capabilities of first responders in attaining information pertaining to unknown environments through the use of UAV. In the past, law enforcement agencies and first responders have faced challenges during emergency events such as earthquakes, tsunamis, fires, floods, and both power and nuclear accidents. One of the major challenges in such situations is acting decisively based on available accurate assessments of disaster sites; however, current UAV platforms have limited capabilities in providing high-quality real-time information under severely unstructured environments. Concerning scenes that possess many hot-spots, such as a fire or nuclear accident, the proposed stereo FLIR camera system may provide an effective tool for first responders to interact and manage the disaster site more effectively.

Traditionally, obstacle avoidance in unstructured environments is done solely with LIDAR or ToF cameras to avoid potential collision with physical obstacles. By considering excessive heat as another obstacle to be avoided, the number of disaster remediation applications for which the system may be effectively implemented drastically increases. The proposed FLIR Cameras will provide information about potential hot-spots in the air in order to protect the vehicle from potential heat damage. The FLIR camera system will identify coordinates of the heat source spatially from the aggregate image center of the body measured in the FLIR camera frame relative to its body-fixed frame. The obstacle avoidance algorithm will then generate a feasible path for the platform to follow, temporarily override the operator's control, and maintain a safe distance from the detected obstacle. Once a safe distance is achieved control is returned to the operator.

2. System Configuration

2.1 UAV platform

The UAV platform was chosen to be a mid-size 650 class quadrotor. Its size allows it to fly indoors and navigate rooms, while offering a relatively large allowable payload. The platform is equipped with Scorpion II 3020 780KV brushless DC motors and 12 x 3.8SF propellers. This high torque propeller/motor pairing provides a maximum lifting force of 32 lbf. excluding the weight of the platform, and promotes a fast mechanical response to a given control input. Our first prototype is shown in Fig. 1.

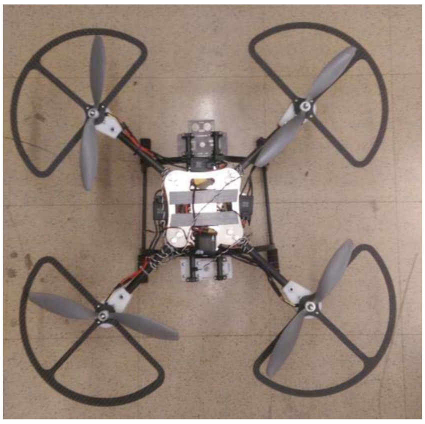

Fig. 1. The UAV platform to be used for Obstacle avoidance.

The frame is made from several plastics, carbon fiber, and aluminum. The two mounting plates were fabricated from 1/16th inch aluminum sheeting using a HAAS CNC Mill. 16mm carbon fiber tubing was used to attach the motor mounts to the mounting plates, and 1/8th inch carbon fiber sheets were used in the fabrication of the propeller guards. Many of the more intricate parts were printed using

978-1-4673-7971-7/15/$31.00 ©2015 IEEE

ABS plastic on an Objet24 3D printer for convenience. These parts include the motor mounts, and adapters for various sensors. The mounting skids and select mounting hardware were purchased commercially. These parts were made from various plastics and composites.

The last design considerations for the UAV platform concern power distribution and basic processing capabilities. While these parts have minimal effect on the platform's flight characteristics, they play a major role in the overall efficiency and performance of the system. For power distribution, four XRotor 50A electronic speed controllers (ESC) were loaded in parallel to a single 8000 mAh 4S Lithium Polymer battery made by Turnigy. The ESC act as three phase inverters whose output is determined via pulse width modulation (PWM). Since the battery operates at a nominal voltage of 14.1V, a single voltage regulator was added to the battery load. The regulator provides DC/DC conversion for 5V devices such as the flight controller, sensors, and onboard computer which was chosen to be an ODROID UX4. The ODROID UX4 is used for all local processes, such as data logging, ground station communications, FLIR camera image processing, and path generation. The device possess a 1.7GHz Exynos 4412 Prime central processing unit (CPU), which is more than sufficient for our purposes, and runs a stripped version of Ubuntu as an Operating System (OS) called Ubuntu 14.04.1 lts (Lubuntu).

2.2 Sensors and Flight Controller

The flight controller for the quadrotor is a 3DR Pixhawk which facilitates both fully autonomous and semi-autonomous operation. To aid in positional tracking and position hold, a PX4 Optical Flow sensor will be used. The Pixhawk interfaces with the ODROID UX4 via USB. Through this interface, telemetry data from the accelerometers, gyroscopes, and barometer can be used in order to aid navigation. A flowchart describing this configuration is show in Fig. 2.

The model of thermal camera to be used is the FLIR Lepton sensor shown in Fig. 3(a). The Lepton sensor is an uncooled microbolometer that detects infrared light of approximate wavelength 8μm to 14 μm. The Lepton has a thermal sensitivity of less than 50 mK, an operating power requirement of 150 mW, a field of view of 51° vertical x 51° horizontal, and an 80 x 60 pixel resolution. The Lepton has an exportable framerate of 9 Hz, and uses an SPI interface to transfer data.

To account for physical obstacles a Hokuyo URG-04LX-UG01 LIDAR sensor will be used in conjunction with the FLIR sensors. The chosen LIDAR scans at 10 Hz over a 240° field of view and possesses an angular resolution of 0.36°. The sensor detects obstacles in a plane roughly parallel to the global frame with the use of a gimbal. This frame possess a known mapping to the platform's body-fixed frame. For further expansion of obstacle avoidance capabilities, a Mesa Imaging SR4000 ToF camera will be integrated to complement the LIDAR. This ToF camera provides a field of view of 43.6° horizontal x 34.6° vertical with a 176 horizontal x 144 vertical pixel depth array.

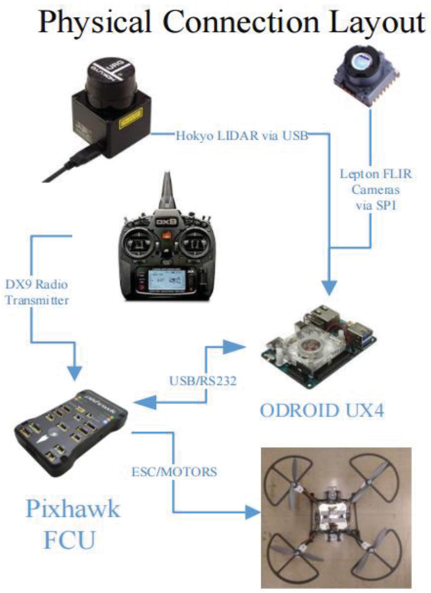

Fig. 2. Physical layout of sensors, onboard computer, and flight controller.

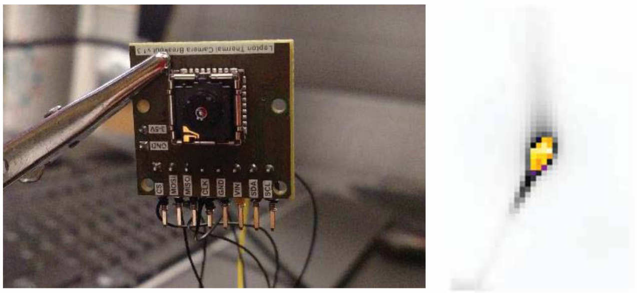

(a)

(b)

Fig. 3. (a) Lepton FLIR sensor mounted within a breakout board (b) FLIR sensor image of lit q-tip

2.2 Robot Operating System

The Robot Operating System [2] (ROS) will be used in order to facilitate communication between all sensors and systems. While ROS generally operates as a publisher/subscriber framework, it also supports standard call and response services as is typical of legacy robotic systems. The ROS framework is an attractive choice for our platform as it drastically reduces development time and the time required to integrate new hardware and system services. Further, ROS has become the de facto platform for modern robotic platforms in recent years, and a wealth of open source libraries have already been developed for a wide variety of devices by the ROS community. For our system, each sensor will have its data published in real time to what is commonly called a topic, while the nodes managing the obstacle avoidance algorithm subscribe to each sensor's topic in order to receive the data required to provide a suitable safe path for a given input. The sensors communicate with the ODROID using ROS over various serial communication interfaces. Fig. 4 shows the data and control flow chart that will be used within ROS.

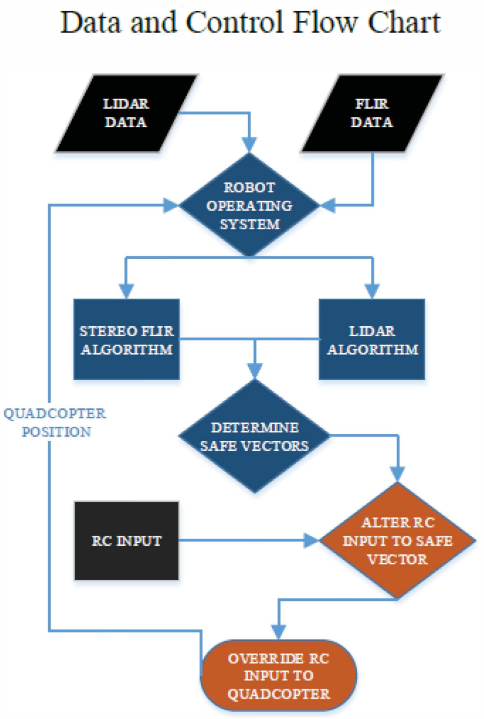

Fig. 4. Data flow within ROS

3. Hot-spot Avoidance Algorithm

3.1 3D Vector Mesh Method

The 3D Vector Mesh (VM) algorithm will be used to avoid hot-spots detected by the proposed stereo FLIR cameras. The method aids in free space navigation around hot-spots existing in typical disaster sites. The proposed algorithm will automatically generate viable flight path vectors, and can be used to overwrite or correct the flight command generated by a remote operator to avoid potential hot-spots existing in the environment. The 3D VM method described in this paper is based on the Vector Field Histogram (VFH) method [1]. This method employs a ToF camera to update three-dimensional range data in real-time. The VFH method achieves obstacle avoidance through a three step algorithm that performs voxel obstacle computation, vector obstacle estimation, and binary mesh representation.

Voxels in this paper refer to 3D spatial units within a 3D grid. Voxel obstacle computation describes the mapping of local obstacles from the received sensor range data measured in a local voxel frame into a universal or global objective voxel frame. Using the transformation described in (1), each identified point of an obstacle in the camera frame {C}, is expressed in the global frame {G}, through the intermediate platform body-fixed frame {U}, where ${}^{\alpha}\boldsymbol{P} \in R^3$ refers to the position of each identified point in some frame α, ${}^{\beta}_{\gamma}\boldsymbol{R}$ defines the rotation matrix mapping of some frame β to some frame γ, and ${}^{\delta}\boldsymbol{P}_{\epsilon}$ describes the position of the origin of the arbitrary frame ϵ with respect to some frame δ.

$$\begin{bmatrix} {}^{G}\boldsymbol{P} \\ 1 \end{bmatrix} = \begin{bmatrix} {}^{G}_{U}\boldsymbol{R}\,{}^{U}_{C}\boldsymbol{R} & {}^{G}_{U}\boldsymbol{R}\,{}^{U}\boldsymbol{P}_{C} + {}^{G}\boldsymbol{P}_{U} \\ 0_{1\times3} & 1 \end{bmatrix} \begin{bmatrix} {}^{C}\boldsymbol{P} \\ 1 \end{bmatrix} \tag{1}$$

The size of the global space is determined by computational cost and the desired accuracy of the modelled environment. A local spherical voxel space is then defined around the UAV with radius R_L. The radius of this space is defined to be very near the maximum visible range of the camera for convenience. If a globally identified obstacle is found to be within the range of this local space, a counter c corresponding to the globally defined voxel containing the coordinate of the obstacle will be incremented.

A smaller spherical voxel space is defined within the first as is shown in Fig. 5 with a small radius R for vector obstacle estimation. This space determines what is called the safe region in which no obstacles may enter. The magnitude of each newly formed element in the set of mapped locally transformed voxels {S} is determined by (2), where $m_{i,j}$ is the magnitude of the vector, $c_{i,j}$ is the incremented value of the (i, j) voxel, and $d_{i,j}$ is the distance between the (i, j) voxel and the origin of the local spherical frame. The set {S} defines a normed measure of safety in a specific direction. Here radial distance to an obstacle loses all meaning. The control parameters $a, b \in \mathbb{R}$ chosen such that $a > 0$, $b > 0$, and $a - bR = 0$, where R is again, the radius of the larger spherical region.

$$m_{i,j} = \left(c_{i,j}\right)^2 (a - bd_{i,j}) \tag{2}$$

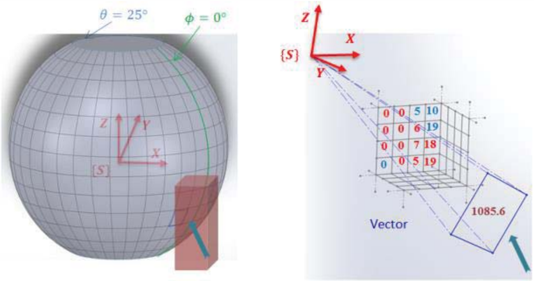

Fig. 5. Vector obstacle computation in mesh sphere space

Binary mesh representation indicated as $M_{i,j}$ replaces the vector obstacle representation in order to improve the efficiency of the algorithm. An experimentally determined threshold η can be applied to determine the elements of this new mesh as described by (3).

$$M_{i,j} = \begin{cases} 1 & if\ m_{i,j} < \eta \\ 0 & if\ m_{i,j} > \eta \end{cases} \tag{3}$$

$$\begin{bmatrix} M_{(i-1,\ j-1)} & M_{(i,\ j-1)} & M_{(i+1,\ j-1)} \\ M_{(i-1,\ j)} & M_{(i,\ j)} & M_{(i+1,\ j)} \\ M_{(i-1,\ j+1)} & M_{(i,\ j+1)} & M_{(i+1,\ j+1)} \end{bmatrix} \equiv \boldsymbol{1}_{3\times3} \tag{4}$$

The directional mesh coordinate (i, j) that satisfies the condition specified in Eq. (4) can be converted to a safe direction denoted (Θ, Φ) in the local spherical coordinate system. The direction objectively considered nearest to the operator's defined target direction will be transformed from the local spherical voxel frame to the UAV body-fixed frame and chosen as the override control input and.

3.2 Simulation Result and Discussion

The simulations described in this paper were implemented in Gazebo [7], an open source simulation environment that supports ROS. A quadrotor model and Kinect sensor defined in pre-built Gazebo libraries were used to test the developed 3D VM method. The interface structure that describes our implementation is shown in Fig. 6. Gazebo models subscribe to published data sent from ROS nodes, and affect the modeled platform's system dynamics within the environment accordingly. The 3D VM algorithm was implemented using three ROS nodes, where each node corresponds to the three main components of the 3D VM method described in this paper.

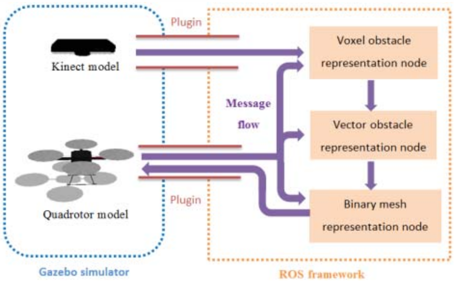
Plugin
Kinect model
Voxel obstacle representation node
Message flow
Vector obstacle representation node
Quadrotor model
Plugin
Binary mesh representation node
Gazebo simulator
ROS framework

Fig. 6. Interface structure between Gazebo and ROS

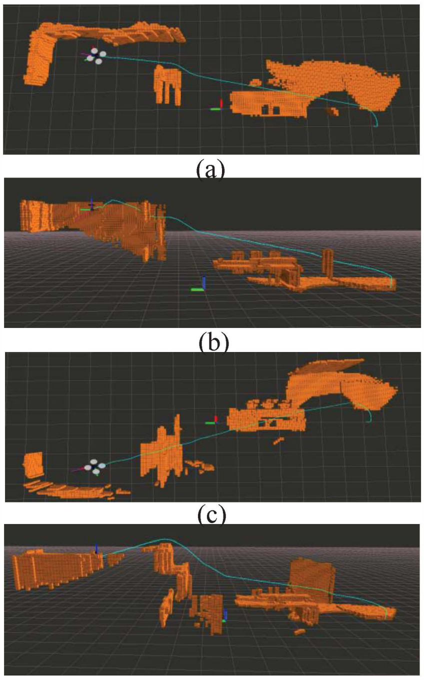

(a)

(b)

(c)

(d)

Fig. 7. Entire paths in simulations. (a) The path of first simulation displayed in XY plane. (b) The path of first simulation displayed in YZ plane. (c) The path of second simulation displayed in XY plane. (d) The path of second simulation displayed in YZ plane.

Two simulations with different initial states and target locations were performed as described in Fig. 7. The modeled UAV was shown to be capable of successfully navigating an unknown environment, while avoiding a variety of obstacles, utilizing conservative changes to its trajectory. In the first case study the UAV was initialized to the global position $(-1.0, -7.0, 0.3)\ m$ with a global target position of $(2.5, 5.0, 3.0)\ m$. The second case study was initialized with starting position $(0.0, -7.0, 0.3)\ m$ and given a global target position of $(-2.5, 5.0, 3.0)\ m$.

In order to analyze performance based on different thresholds 4 simulations were used using threshold values of 0.20, 0.25, 0.30 and 0.35. The simulation results in demonstrate successful navigation in all cases with no collision. Fig. 8 shows the implementation of the different thresholds used, and compares the generated paths determined by the 3D VM method for the quadcopter. In general, a smaller threshold promotes larger oscillations in the generated paths.

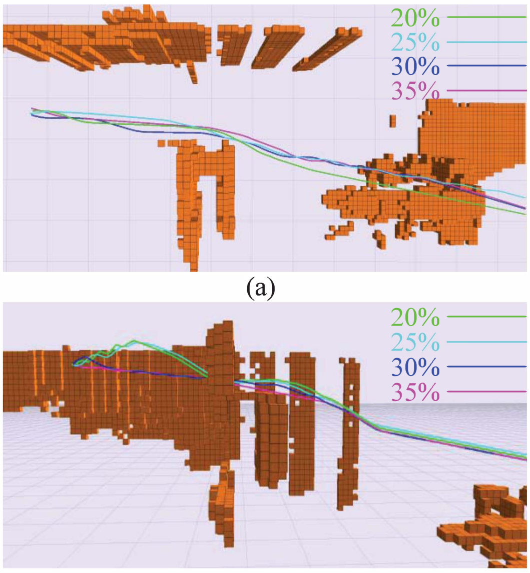

(a)

(b)

Fig. 8. Differences of paths based on various threshold values from eq. (3).

3.3 Hot-spot Avoidance Method

In the platform's prescribed semi-autonomous state, an RC input described by the operator will be used to establish a goal vector for the platform. In the case of an impending collision, the onboard obstacle avoidance system will alter the platform's trajectory using the 3D VM algorithm in order to avoid physical obstacles or hot-spots in the platform's path.

To process data received from the two Lepton FLIR cameras, a disparity map will be made from the two FLIR images. The safe operational temperature range for a quadrotor will be used to determine a threshold for the disparity map. Any hot-spot with temperatures exceeding this threshold will be interpreted as an obstacle and its spatial coordinates will be fed into the 3D VM algorithm for avoidance measures.

The ToF camera and LIDAR will be used to provide the 3D VM avoidance algorithm with essential point cloud data needed for solid obstacle avoidance. This, in conjunction with the heat obstacle data provided by the FLIR sensors, will allow the algorithm to determine an optimum path. These vectors can then be given to the flight controller for path planning.

4. Conclusion

The paper describes hardware and software components needed for developing a small UAV effectively used by first responders in typical disaster sites involving fires. A stereo thermal camera is used to locate and avoid heat sources that can potentially damage UAV's sensitive electronic and structural components. The goal is to have first responders easily operate UAVs semi-autonomously to gather information, and act decisively. Based on the results obtained from computer simulation, the proposed hardware/software components have a strong potential to accomplish this goal in typical disaster remediation tasks.

Acknowledgements

The authors acknowledge the financial support from National Science Foundation Partnerships for Innovation-PFI through University of Nevada, Reno, Award No. IIP-1430328.

References

[1] Borenstein, I., and Koren, Y., "The Vector Field Histogram – Fast Obstacle Avoidance for Mobile Robots", IEEE Journal of Robotics and Automation, Vo1.7, No.3, June 1991, pp.278-288.

[2] http://www.ros.org/

[3] Matthies L., Brockers R., Kuwata Y. and Weiss S. "Stereo vision-based obstacle avoidance for micro air vehicles using disparity space", IEEE International Conference on Robotics and Automation, Hong Kong, China, pp. 3242-3249, 2014.

[4] Stefan Hrabar, "3D Path Planning and Stereo-based Obstacle Avoidance for Rotorcraft UAVs", 2008 IEEE/RSJ International Conference on Intelligent Robots and Systems, Acropolis Convention Center, Nice, France, Sept, 22-26, 2008

[5] Ulrich I., and Borenstein J. "VFH+: Reliable Obstacle Avoidance for Fast Mobile Robots", in Proceedings of the IEEE International Conference on Robotics and Automation, Vol. 2, Leuven, Belgium, pp. 1572-1577, May 1998.

[6] Yue H., Chen W., Wu X., and Zhang J. "Kinect Based Real Time Obstacle Detection for Legged Robots in Complex Environments", IEEE 8th Conference on Industrial Electronics and Applications (ICIEA), Melbourne, Australia, pp. 205-210, June 2013.

[7] http://gazebosim.org/